Variation in Root System Architecture Response to Arsenic during Establishment and Onset of Storage Root Formation in Two Sweetpotato (*Ipomoea batatas* L.) Cultivars

Arthur Villordon

Louisiana State University Agricultural Center, Sweet Potato Research Station, Chase, LA 71324, USA

Jack Baricuatro

Department of Chemistry and Physics, Louisiana State University-Shreveport, Shreveport, LA 71115, USA

Abstract. The primary objective of this work was to generate species-specific information about root architectural adaptations to simulated natural levels of arsenic (As) during the establishment phase and onset of storage root formation in sweetpotato. Cultivars Bayou Belle and Beauregard were grown on sand substrate and provided with 0.5X Hoagland's nutrient solution with varying levels of As (0, 5, 10, or 15 mg·L^{-1}). During the first experiment, entire root systems were sampled at 5, 10, and 15 days, corresponding to key adventitious root developmental stages. Compared with the untreated controls at 15 days, 'Bayou Belle' and 'Beauregard' provided with 15 mg·L^{-1} As showed respective increases in the following root architectural attributes: 168% and 130% in main root length; 168% and 98% in lateral root length; and 140% and 50% in lateral root density. A second experiment was performed to produce storage root samples at 50 days. Storage root length, width, and length/width ratio did not vary with As levels. The accumulation of As in storage roots increased with increasing As levels. The results support the hypothesis that natural As levels stimulate adventitious root development in sweetpotato in a cultivar-dependent manner. The observations are consistent with findings of other species that show similar growth stimulation at low As levels. This is the first report of sweetpotato root system architecture responses to experimental levels of As that are known to be present in agricultural soils. Standardization of experimental procedures and understanding of root system adaptations to natural levels of As could lead to a more systematic exploitation of genome-wide techniques and characterization of the molecular basis of reduced As uptake in plants.

Arsenic (As) is a toxic metalloid that is widely distributed in the environment as a result of natural and anthropogenic activities (Punshon et al. 2017). Despite its status as a nonessential element, plants can take up As via transporters, leading to accumulation in edible portions of crop plants and eventual transfer to the food chain. Arsenic V is the dominant species in aerobic soils. Because it is structurally analogous to phosphate (Pi), it enters plant roots via Pi transporters (Tang and Zhao 2021). Both As and Pi have nearly identical pK$_a$ values and similar ionic radius and charge characteristics, rendering it difficult for proteins to distinguish the two anions (Elias et al. 2012; Tawfik and Viola 2011). Exposure of crop plants to As above the threshold limit in soil or in irrigation water results in an array of adverse effects, including wilting, curling, necrosis of leaf blades, reduced root elongation, proliferation, and nodulation (Chandrakar et al. 2016). Current evidence suggests that the permissible limit of As is 20 mg·kg^{-1} in agricultural fields; however, for sensitive plants, even 5 mg·kg^{-1} is injurious (Panda et al. 2010). The worldwide mean concentration of As in soil is 10 mg·kg^{-1} (Piršelová et al. 2022). In contaminated orchard lands associated with the historical use of lead arsenate pesticides, soil As ranges from 20 to 250 mg·kg^{-1}. In addition to being toxic, As limits plant uptake of minerals that are essential for human health, such as iron and zinc (Brackhage et al. 2014; Duan et al. 2013).

It is necessary to understand how plants respond to natural levels of As and other toxic elements to develop management practices for food safety and human health. Recent evidence from model plants and well-studied crop species revealed that As reshapes the spatial configuration of roots in thale cress (*Arabidopsis thaliana*) (Kumar et al. 2020; Piacentini et al. 2020), pigeon pea (*Cajanus cajan*) (Pita-Barbosa et al. 2015), peanut (*Arachis hypogea*) (Bianucci et al. 2017), and rice (*Oryza sativa*) (Ronzan et al. 2019; Wang et al. 2018), among others. The presence of As exerts a profound effect on root architecture that is tightly coordinated with the detoxification machinery (Navarro et al. 2022). In sweetpotato, the successful emergence and development of lateral roots, the main determinant of root system architecture (RSA), determine the competency of adventitious roots (ARs) to undergo storage root formation (Villordon et al. 2012). Hence, knowledge about intrinsic and environmental variables that control RSA development contribute to the understanding of storage root formation in this globally important root crop. There were two main objectives. First, information about RSA modifications to natural levels of As will provide insights about adaptations of existing sweetpotato cultivars to As levels. Second, this study can be adapted to provide a method of screening germplasm tolerance to As and other toxic elements.

Materials and Methods

Plant materials and experimental conditions. The greenhouse experiments were performed at the Louisiana State University Agricultural Center Sweet Potato Research Station, in Chase, LA, USA (32°6′N, 91°42′W). Two-pot experiments with two replicate studies per experiment were conducted (Table 1). The first experiment was established to measure RSA attributes at three timepoints, 5, 10 and 15 d (Table 1). The second experiment involved measuring storage root attributes and As accumulation in storage roots at 50 d (Table 1). The Beauregard (BX) (Rolston et al. 1987) and Bayou Belle' (BB) (LaBonte et al. 2013) cultivars were used; BX is a copper-skin, orange-flesh cultivar that is grown globally, and BB is a red-skin, orange-flesh cultivar that was released specifically for processing. Virus-tested generation 1 storage roots were bedded in plastic containers containing soilless media (Sungro; Sun Gro Horticulture, Bellevue, WA, USA) and served as a source of transplants or vegetative cuttings for subsequent experiments. During each experiment, cuttings were set in 10-cm-diameter polyvinyl chloride pots (height, 30 cm) with detachable plastic

Table 1. List of experiments.

Expt.	Study	Date planted	Date(s) harvested	Measurements/timepoints
1	A	20 Jan 2023	25 Jan 2023	Adventitious root count, lateral root length,
			30 Jan 2023	lateral root density;
			4 Feb 2023	5, 10, and 15 d
	B	23 Feb 2023	28 Feb 2023	
			5 Mar 2023	
			11 Mar 2023	
2	A	20 Jan 2023	10 Mar 2023	Storage root length, width, length/width ratio,
	B	23 Feb 2023	14 Mar 2023	arsenic accumulation;
				50 d

bottoms. Each plastic bottom had five drain holes (diameter, 2 mm). Additionally, each polyvinyl chloride pot had four rows of side drain holes (diameter, 2 mm; 3-cm within-row spacing) that were located diametrically opposite each other. These side drain holes were added to help reduce the incidence of a perched water table (Bilderback and Fonteno 1987). Washed river sand was used as a growth substrate for all experiments. The diameter of the sand particles varied from 0.05 to 0.9 mm, with the majority (83%) in the range of 0.2 to 0.9 mm. Substrate samples were submitted for laboratory analyses (Environmental Hazards Services, Richmond, VA, USA), and As was below detectable levels (detection limit: 0.02 mg·L^{-1}). During all experiments, vegetative terminal cuttings with the following characteristics were used: length of 25 30 cm; five to six fully opened leaves; diameter of ~5 mm at the basal cut; and uniform distribution of nodes.

All pots were provided with 0.5X Hoagland's No. 1 solution (nitrate only; control) (Hoagland and Arnon 1950) or containing 5, 10, and 15 mg·L^{-1} As applied as sodium monohydrogen arsenate (Na$_2$HAsO$_4$·7H2O). These treatment levels were meant to simulate natural conditions based on available information. First, the worldwide mean concentration of As in soil is 10 mg·kg^{-1} (Piršelová et al. 2022). Second, unpublished As sampling data from commercial production fields in Louisiana showed a range of 2 to 15 mg·L^{-1} and mean of 7.3 mg·L^{-1} (Sistrunk M, personal communication). During the critical establishment stage (first 3 d), 150 mL of the nutrient solution was provided daily. After establishment, 200 mL was provided every other day until the completion of the study. This protocol is the equivalent to providing 25 mm·ha^{-1} of water with each application. Cuttings were planted to a uniform depth of 6 cm with two (BX) to three (BB) nodes under the growth substrate surface, depending on the cultivar. All experiments were arranged as a randomized complete block repeated across planting dates. Unless otherwise indicated, there were four replicates in each experiment (one plant per pot = one replicate).

Growth substrate moisture was measured with ECH2O soil moisture sensors inserted vertically at a depth of 2 to 7 cm (Model EC-5; Decagon Devices Inc., Pullman, WA, USA). The moisture of the growth substrate ranged from 5% to 9% volumetric water content, with $\approx50\%$ of field capacity equaling 7% volumetric water content. At saturation, the growth substrate typically ranged from 12% to 14% volumetric water content (Villordon et al. 2012). The greenhouse temperature regime for the first planting date was 28 °C (SD, 2.3) for 14 h (day) and 24 °C (SD, 3.3) for 10 h (night). The average relative humidity (RH), which was measured hourly, was 59% (SD, 13.4). The temperature regime for the second planting date was 31 °C (SD, 2.2) for 14 h (day) and 27 °C (SD, 2.7) for 10 h (night). The average RH was 53% (SD, 15.7). The temperature and RH were monitored at the canopy level using an integrated temperature and RH sensor (Model RHT; Decagon Devices Inc.). Supplementary lighting was provided using light-emitting diode grow lights (Lumigrow Inc., Emeryville, CA, USA) for 14 h per day. Photosynthetic photon flux for the first planting date ranged from 422 to 2731 mmol·m^{-2}s^{-1}, and photosynthetic photon flux for the second planting date ranged from 582 to 3770 mmol·m^{-2}s^{-1}. Photosynthetic photon flux was measured at the canopy level with a quantum sensor (Model QSO-S; Decagon Devices Inc.). These experimental approaches have been used to validate storage root initiation timing in BX (Villordon et al. 2009, 2012) and measure root architecture responses to biotic and abiotic variables (Villordon et al. 2012, 2013; Villordon and Clark 2014, 2018).

Root architecture measurements. With each sampling, the detachable plastic bottoms were removed, the pot was tilted, and the growth substrate was gradually removed using a stream of water. Then, the roots were placed in water-filled trays and rinsed twice. The AR samples were stored in 50% ethanol solution before scanning. Storage root formation was confirmed by verifying the onset of anomalous cambium development in representative BX adventitious root samples with a diameter ≥2 mm (Villordon et al. 2020).

Measurement of root architectural attributes followed the procedures described in prior work (Villordon et al. 2020). Briefly, intact washed ARs were floated on waterproof trays and scanned using an Epson Perfection V850 Pro Photo Scanner (Epson Corporation, CA, USA). The image acquisition parameter was set to "high" accuracy (600 dpi; image size, ≈18 MB), whereas analysis precision was set to "high."

According to prior work using the cultivar BX, preset intervals were used to classify root classes (Villordon et al. 2012, 2013). However, the variation in complexity of root samples among cultivars and overlapping root thickness led to classification errors among root classes in the current study. Hence, the following modifications of prior approaches were adopted for this work. For the purpose of this work, AR specimens (with labeled sections in Fig. 1) were used to standardize terminologies and clarify specific root class categories and attributes measured. First, the main (or primary) root length (MRL) (Fig. 1A−C) was manually measured using the segmented line feature in ImageJ (Schneider et al. 2012). Second, the total root length (TRL) was measured using Rhizovision Explorer (Seethepalli and York 2020). Debris such as sand particles and loose root tissue were excluded from the analysis by turning on the filter for nonroot objects in RhizoVision Explorer (size, 25 pixels). Finally, the lateral root length (Fig. 1A−C) was calculated by subtracting the manual MRL measurements from the TRL.

Storage root shape measurements and arsenic analysis. Storage roots sampled at 50 d were photographed and images were digitally analyzed using ImageJ (Schneider et al. 2012). The segmented line feature was used to measure the storage root length, whereas the straight-line feature was used to measure the storage root diameter. The length/width ratio was subsequently calculated. Storage roots were washed with deionized water and sent to Brooks Applied Laboratories (WA, USA) for the As bulk analysis (unpeeled).

Statistical analysis. All quantitative and count data were transformed using log 10 and square root transformation, respectively. Ratios were As-transformed. Statistical analyses of transformed values were performed using SAS Proc Mixed (SAS 9.4; SAS Inc., Cary, NC, USA). Fisher's least significant difference test ($P = 0.05$) was used to test for statistical significance. We failed to detect a significant planting date and cultivar effects on all root attributes; hence, data were combined. The R package ggplot2 (Wickham 2009) was used to generate boxplots using R Studio (version 1.2.1335; R Studio Inc., Boston, MA, USA) with R version 3.6 (R Development Core Team 2019). The data presented were nontransformed data.

Results and Discussion

Adventitious root number. Sweetpotato commercial propagation and storage root formation depend on the successful emergence of ARs from vegetative cuttings. The ARs emerge from preformed nodes or basal cut ends as early as 3 to 5 d, depending on the cultivar (Ma et al. 2015; Villordon et al. 2009). At 5 d, there were no differences in the AR number within cultivars and across As levels (Fig. 2A). At 10 d, 15 mg·L^{-1} As suppressed the AR number by 80% relative to the control for the cultivar BX (Fig. 2B). A similar trend was observed for the cultivar BB. This trend continued at 15 d (Fig. 2C). Relatively limited information is available for As effects on AR emergence in other plant or crop species. Tripathi et al. (2021) reported that 15 mg·L^{-1} As suppressed AR
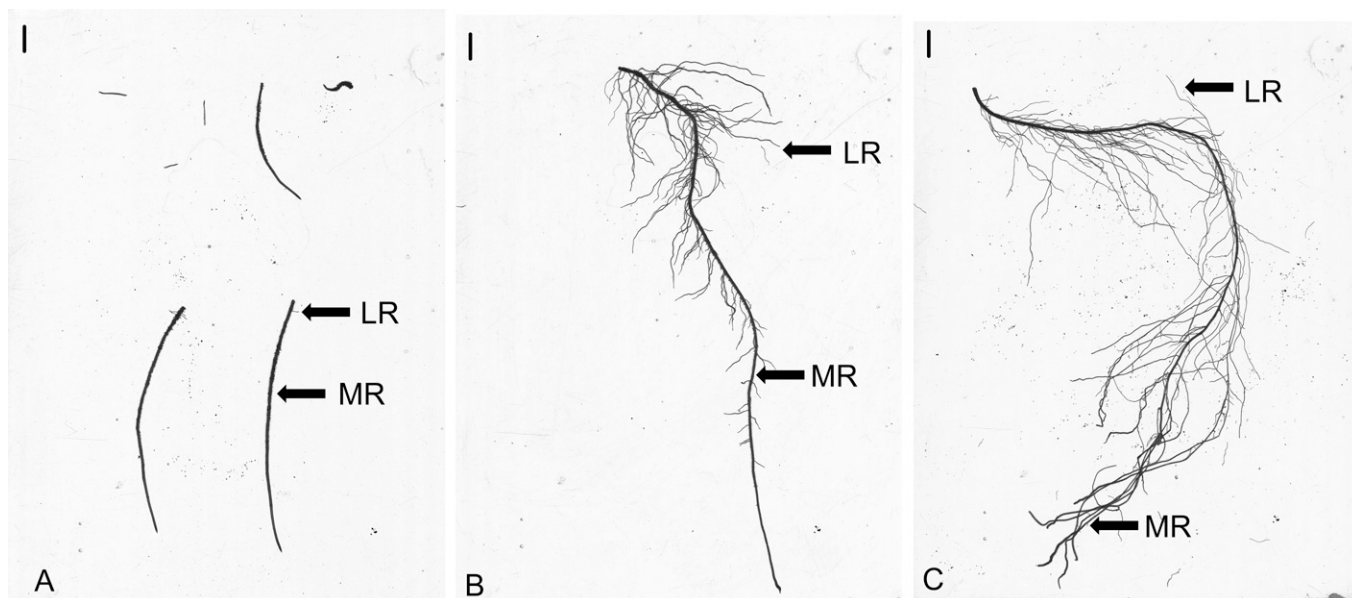
Fig. 1. Sweetpotato cultivar 'Bayou Belle' adventitious roots sampled at 5 (**A**), 10 (**B**), and 15 d (**C**) from plants grown in control conditions. Adventitious roots in (**A**) represent all adventitious roots sampled from one plant. A main root (MR) and first-order lateral root (LR) are labeled in each plate to clarify the terminology used throughout this report. Scale bar = 1 cm.

development in rice that was mitigated by the addition of silicon. Srivastava et al. (2019) reported a reduction in the AR number of rice plants grown in 10 mg·L^{-1} As.

The AR number variation at establishment among sweetpotato cultivars has been reported previously (Lowe and Wilson 1974; Nakatani and Watanabe 1986). Additional ARs emerge over the next 10 d depending on genotype and environmental conditions (Lowe and Wilson 1974). Evidence from prior work (Lowe and Wilson 1974; Ma et al. 2015) indicated that there is no direct correlation between the total AR number per plant and final storage root number at harvest in sweetpotato. Lowe and Wilson (1974) cited limiting factors that influenced final storage root yield, including assimilate production and transport. We have previously documented that cultivar-specific AR emergence is mediated by differential ethylene sensitivity in cultivars (Villordon et al. 2012). There is evidence that ethylene regulates the As

stress response in root systems in *Arabidopsis* (Singh et al. 2021) and rice (Huang et al. 2012).

Main root length. The MR length did not vary at 5 d (Fig. 3A). However, 15 mg·L^{-1} As was associated with 91% and 119% increases in the MR length at 10 d in BB and BX, respectively (Fig. 3B). At 15 d, 15 mg·L^{-1} As was associated with 168% and 130% increases in the MR length of cultivars BB and BX, respectively (Fig. 3C). Findings of other species showed that the MR length varied according to As levels. Evans et al. (2005) reported that 0.1 mg·L^{-1} As stimulated the MR length. Evans et al. (2005) further documented that maize roots grown on medium containing As suppressed the growth of roots grown with phosphate (P) only. They concluded that in some situations, and at very low levels, As may stimulate root growth, ultimately leading to a selective advantage for plants that exhibit such behavior. Rai et al. (2011) reported increases in root length when *Artemisia annua*

was grown in 0 to 3 mg·L^{-1} As. *A. annua* has been shown to be tolerant to As stress (Kumari et al. 2017; Rai et al. 2011). Piacentini et al. (2020) reported that 20 mg·L^{-1} As increased the MR length of *Arabidopsis*. Spagnoletti and Lavado (2015) reported that 25 and 50 mg·L^{-1} As progressively reduced the MR length of soybeans (*Glycine max*), and this effect was reversed by mycorrhizal colonization. Xu et al. (2015) reported the reduction of *Arabidopsis* primary roots when wild-types were grown in 5 mg·L^{-1} As, and no reduction in a NIP3;1 loss-of-function mutant. NIP3;1 is a member of As III transporters that functions in the uptake and root-to-shoot translocation of As III (Xu et al. 2015).

Lateral root length. The lateral root (LR) length did not vary at 5 d for both cultivars and across As levels (Fig. 4A). However, the LR length of BB and BX increased 168% and 130%, respectively, at 15 mg·L^{-1}, relative to the untreated control at 10 d (Fig. 4B).
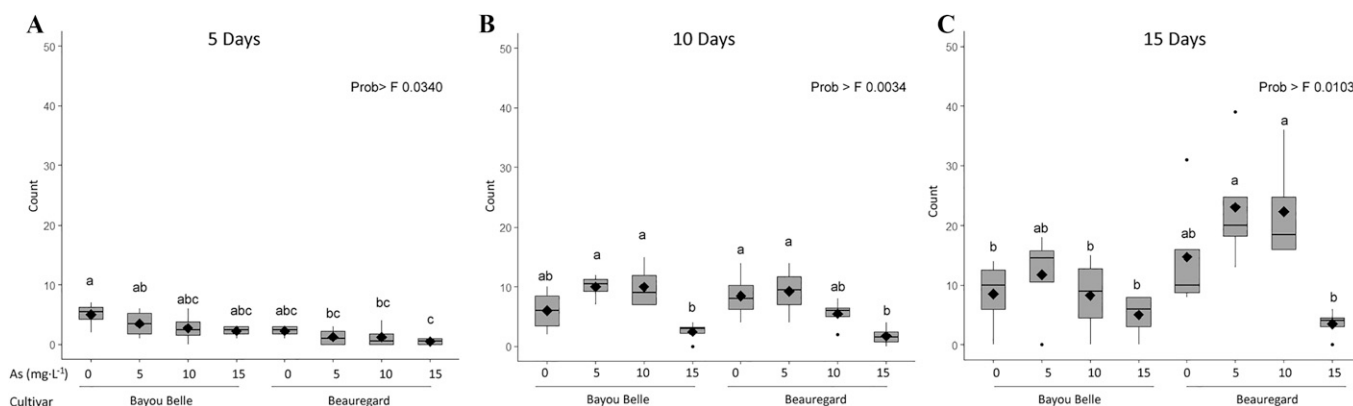

Fig. 2. Box plots of adventitious root number in sweetpotato cultivars grown in four arsenic levels from two planting dates. Boxes represent the interquartile range (IQR; or middle 50%) of values for each feature. Shaded diamonds represent mean values. Bold horizontal lines indicate median values. Upper box plot whiskers represent the last data point within the range of the 75% quantile + 1.5 IQR. Lower box plot whiskers represent the last data point within the range of the 25% quantile − 1.5 IQR. Dots represent outliers (values smaller or larger than the median ± 1.5-times the IQR). Boxes with different letters are significantly different based on Fisher's least significant difference mean separation test ($P < 0.05$).
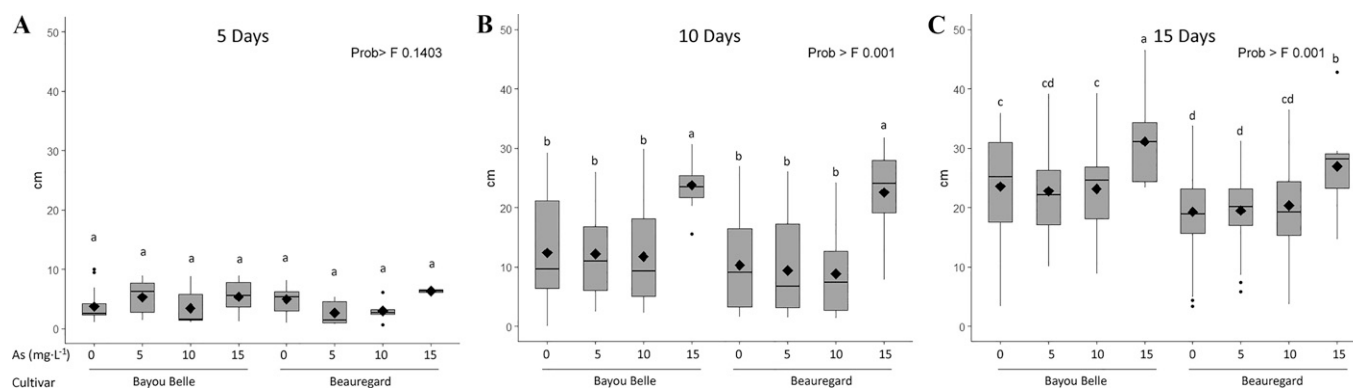
491

Fig. 3. Box plots of the main root length of sweetpotato cultivars grown in four arsenic levels from two planting dates. Boxes represent the interquartile range (IQR; or middle 50%) of values for each feature. Shaded diamonds represent mean values. Bold horizontal lines indicate median values. Upper box plot whiskers represent the last data point within the range of the 75% quantile + 1.5 IQR. Lower box plot whiskers represent the last data point within the range of the 25% quantile − 1.5 IQR. Dots represent outliers (values smaller or larger than the median ± 1.5-times the IQR). Boxes with different letters are significantly different based on Fisher's least significant difference mean separation test ($P < 0.05$).

At 15 d, there were 143% and 32% increases in the LR length of BB and BX, respectively (Fig. 4C). Current available data show conflicting As effects on the LR length. Piacentini et al. (2020) documented that 20 mg·L^{-1} As was associated with *Arabidopsis* LR growth promotion. In contrast, 8 mg·L^{-1} As-induced reductions in LR length have been reported for rice (Srivastava et al. 2019). Pita-Barbosa et al. (2015) reported that 1.5 mg·L^{-1} As was associated with reductions in the LR length and number in *Cajanus cajan* grown in hydroponic conditions (Pita-Barbosa et al. 2015).

In model plants and well-characterized crop species, LR length variation is associated with biotic and abiotic variables. For maize, the LR length is dictated by the relative availability of nitrogen (N) and P (Postma et al. 2014). The LR length increased with increasing N/P ratios in winter wheat (*Triticum aestivum*) (Adalsteinsson and Jensén 1988); however, Griffiths et al. (2022) observed that the LR length decreased under low N. This variation in response to N availability is likely associated with variations in genetic responses to N availability (Zhe et al. 2023). Other variables associated with an increased LR length include salinity for *Plantago maritima* (Rubinigg et al.

2004), increased soil temperature for peanut (*Arachis hypogea* L.) (Golombek and Johansen 1997), and mycorrhizal colonization for spruce (*Picea abies*) (Wagner et al. 2016). For sweetpotato, we have previously documented that the LR length increased in a genotype-specific manner as a result of *Meloidogyne incognita* infection (Villordon and Clark 2018) and increased N availability (Villordon et al. 2013).

Lateral root density. The LR density remained relatively similar among cultivars and across As levels during the first 10 d, except for a slight increase in the LR density at 5 d for BX grown in 10 mg·L^{-1} relative to the control (Fig. 5A and B). At 15 d, there were 140% and 50% increases in the LR density of BB and BX, respectively, in plants grown with 15 mg·L^{-1} As relative to the controls (Fig. 5C). Piacentini et al. (2020) reported similar results for *Arabidopsis*, where As exposure to 25 mg·L^{-1} As was associated with increased primary root length and LR density. Ronzan et al. (2019) reported that 40 mg·L^{-1} As reduced the LR density of the wild-type rice, but not in a mutant for jasmonate biosynthesis, supporting the hypothesis that the genotype plays a role in RSA adaptations. Available evidence shows that the LR density

is associated with the competency of the AR to become a storage root (Villordon et al. 2012). Optimal LR development enables the plant to gain better access to soil-based resources to support plant growth and storage root development (Gregory and Wojciechowskic 2020). However, relatively limited information is available about intrinsic and external variables that influence the LR density of sweetpotato. First, just like in model systems and well-studied crop species, it has been demonstrated that reduced substrate moisture availability and N availability reduce the LR density (Villordon et al. 2012). Second, available P levels were associated with variations in the LR density across sweetpotato cultivars (Villordon et al. 2020), corroborating findings of model systems and well-studied crop species. In particular, although BB consistently showed increased LR density with increasing P availability, the cultivar Okinawa showed increased LR density with decreasing P (Villordon et al. 2020). For *Arabidopsis*, it has been demonstrated that LR density can vary depending on available P in the growth medium (López-Bucio et al. 2002; Williamson et al. 2001).

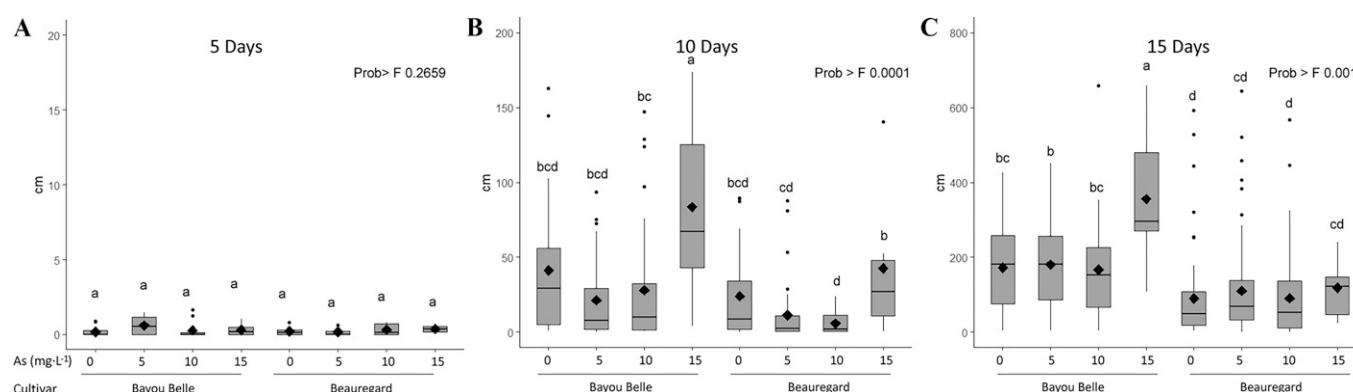The experimental results from this work corroborate a key finding of other plant and

Fig. 4. Box plots of the lateral root length of sweetpotato cultivars grown in four arsenic levels from two planting dates. Boxes represent the interquartile range (IQR; or middle 50%) of values for each feature. Shaded diamonds represent mean values. Bold horizontal lines indicate median values. Upper box plot whiskers represent the last data point within the range of the 75% quantile + 1.5 IQR. Lower box plot whiskers represent the last data point within the range of the 25% quantile − 1.5 IQR. Dots represent outliers (values smaller or larger than the median ± 1.5-times the IQR). Boxes with different letters are significantly different based on Fisher's least significant difference mean separation test ($P < 0.05$).
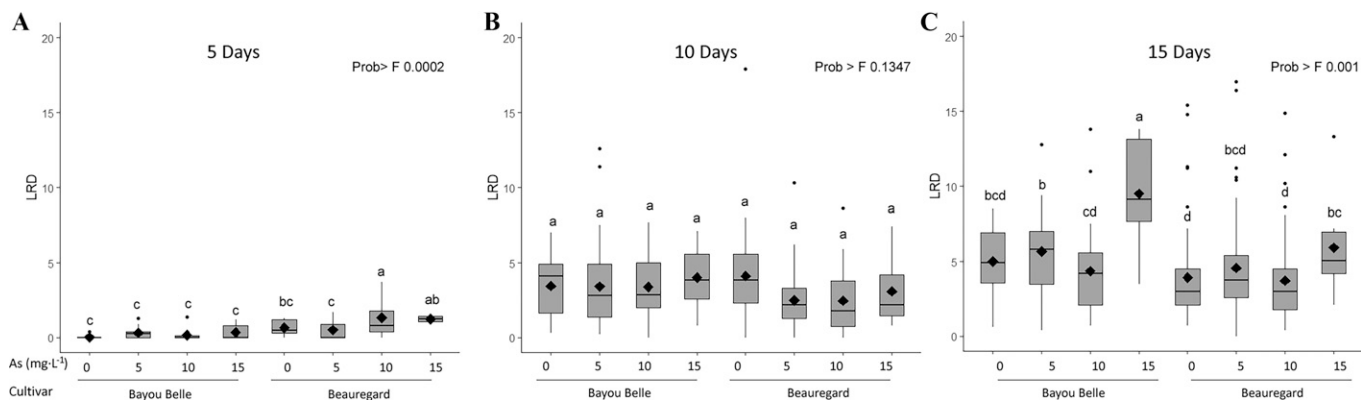
Fig. 5. Box plots of the lateral root density of sweetpotato cultivars grown in four arsenic levels from two planting dates. Shaded diamonds represent mean values. Bold horizontal lines indicate median values. Boxes represent the interquartile range (IQR; or middle 50%) of values for each feature. Upper box plot whiskers represent the last data point within the range of the 75% quantile + 1.5 IQR. Lower box plot whiskers represent the last data point within the range of 25% quantile − 1.5 IQR. Dots represent outliers (values smaller or larger than the median ± 1.5-times the IQR). LRD = lateral root density. Boxes with different letters are significantly different based on Fisher's least significant difference mean separation test ($P < 0.05$).

crop species: low levels of As are associated with the stimulation of root growth as manifested through root architectural modifications (Evans et al. 2005; Piršelová et al. 2022). This work also corroborates the work of Navarro et al. (2022), who reported that studying how roots transduce As perception into root morphological responses integrated with tolerance mechanisms is an urgent matter. The experimental As levels used during this work were based on available data from commercial sweetpotato production fields. A range of 3.5 to 13 mg·L^{-1} As (unpublished data) was detected by a 2-year repetitive sampling of research fields at the Louisiana State University Agricultural Center Sweet Potato Research station, where sweetpotato cultivar development has been ongoing since 1948, and where the cultivars used in the current study were initially selected (LaBonte et al. 2013; Mulkey and Hernandez 1994; Rolston et al. 1987). Considering the available data, we hypothesized that current sweetpotato cultivars used in this work as well as others that have been bred under similar conditions have the inherent ability to tolerate As levels associated with stimulating root growth. Evans et al. (2005) arrived at the same conclusion, and reported that, in some situations and at very low levels, As may stimulate root growth, ultimately leading to a selective advantage for plants that exhibit such behavior. There are conflicting reports about the role of As in root development. Aside from nonstandard As levels used for experimental treatments, Navarro et al. (2022) cited nonuniform experimental conditions that could render As availability lower, allowing the plant to detoxify the As, increasing its accumulation and leading to variability in RSA responses. At the same time, other reasons were cited for selecting the experimental As level and were frequently species-specific concentrations that inflict damage on soybean (Spagnoletti and Lavado 2015) and damage plants but do not completely inhibit the growth of *Arabidopsis* root system (Piacentini et al. 2020) and meet the LD50 dose of arsenate for selected rice cultivars (Srivastava et al. 2019). This underscores the importance of

conducting species-specific studies to generate baseline information about As effects on the root system. In particular, any perturbations during the first 15 d of sweetpotato RSA development directly influences the storage root yield and quality of sweetpotato (Gregory and Wojciechowskic 2020). This enables further experimental work involving sweetpotato that is necessary to translate key findings from model systems and other well-studied crop plants. Based on the available evidence, it appears that P and its role in RSA modifications and As uptake is a priority for follow-up investigations. For example, cumulative evidence from model systems and well-studied crop species support the hypothesis the P exerts a significant influence on As mobility and bioavailability (Bolan et al. 2013; Khattak et al. 1991; Tu and Ma 2003; Wu et al. 2022). Additionally, Wang et al. (2018) presented evidence that OsWRKY28, a group IIa WRKY gene, regulates P and As accumulations, which are involved in root architectural modifications. WRKYs are transcriptional factors involved in stress tolerance, and prior work involving rice (Chakrabarty et al. 2009) has shown that arsenate exposure upregulated OsWRKY28 expression.

Storage root responses and As accumulation. There were no differences in the storage root length, diameter, length/width ratio, and count at 50 d for both cultivars (Table 2). These findings support the hypothesis that

current cultivars used in this study, as well as other cultivars bred in similar conditions, possess an inherent adaptation to low As levels. However, additional studies are needed to determine the role of cultivar-specific P requirements in As uptake by the sweetpotato root system. The presence of As in storage roots at 50 d in response to As treatments shows a dose-dependent response (Fig. 6), similar to that reported for *Allium cepa* (Gupta et al. 2018), rice (Dixit et al. 2016), and *A. annua* (Rai et al. 2011). The relative increase in accumulation of As appears to be similar across cultivars. Therefore, an experimental approach can be adapted toward screening and testing management approaches for reducing As uptake. For example, P treatments and substrate amendments can be incorporated as part of these experimental mitigation strategies. The storage roots can be sampled at 50 d and provide sufficient storage root mass for As analyses.

Conclusion

This is the first report of sweetpotato root system architecture responses to experimental levels of As that are known to be present in agricultural soils. The apparent stimulation of root development at low As levels corroborate some findings in model systems and well-characterized crop species. Conflicting results from other studies underscore the

Table 2. Storage root attributes and count at 50 d for sweetpotato cultivars Bayou Belle and Beauregard grown with natural levels of arsenic (As).

Cultivar	As (mg·L^{-1})	Length	Diam	Length/width	Count
Bayou Belle	0	6.9 ± 0.4 a	1.9 ± 0.1 a	3.8 ± 0.2 a	4.5 ± 0.9 a
	5	7.1 ± 0.4 a	1.9 ± 0.2 a	4.0 ± 0.4 a	3.8 ± 0.3 a
	10	7.5 ± 0.3 a	1.8 ± 0.1 a	4.6 ± 0.5 a	4.3 ± 0.3 a
	15	7.2 ± 0.5 a	1.8 ± 0.1 a	4.2 ± 0.4 a	4.0 ± 0.7 a
Beauregard	0	6.9 ± 0.5 a	1.7 ± 0.1 ab	4.2 ± 0.2 a	5.3 ± 0.5 a
	5	6.1 ± 0.5 ab	1.5 ± 0.1 ab	4.3 ± 0.4 ab	4.3 ± 0.8 a
	10	6.9 ± 0.5 a	1.6 ± 0.2 ab	5.0 ± 0.5 a	4.3 ± 0.3 a
	15	5.2 ± 0.5 b	1.4 ± 0.1 b	3.9 ± 0.3 b	5.5 ± 0.9 a

Values represent means (±*SE*). Means within columns followed by a common letter are not significantly different based on Fisher's least significant different means separation test ($P \leq 0.05$). Values were log10-transformed. Corresponding nontransformed values are shown. Storage root samples were collected 50 d after planting.
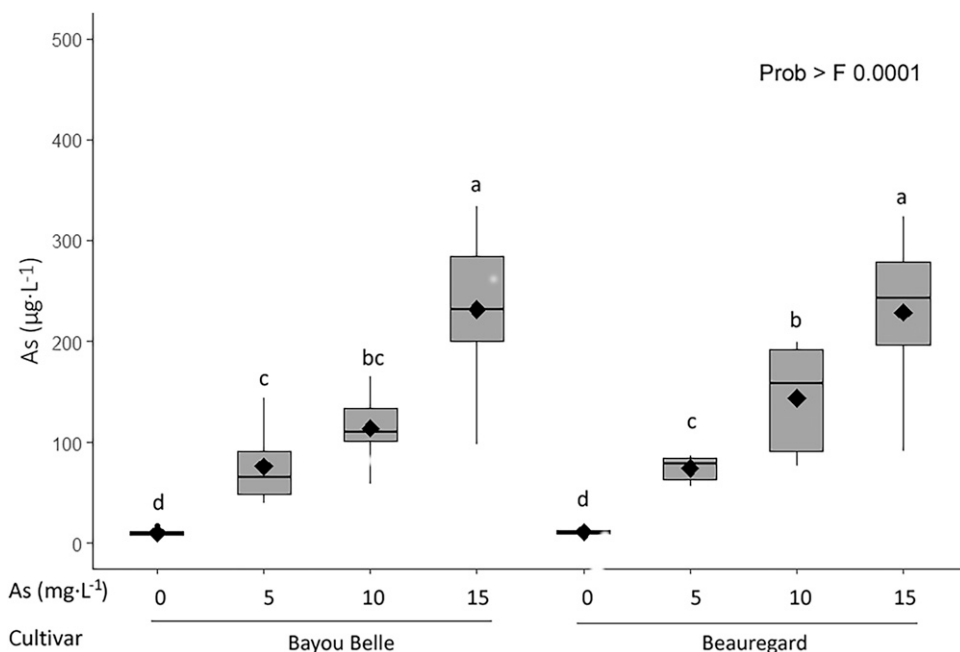
Fig. 6. Box plots of the arsenic presence of sweetpotato cultivars grown in four arsenic levels from two planting dates. Shaded diamonds represent mean values. Bold horizontal lines indicate median values. Boxes represent the interquartile range (IQR; or middle 50%) of values for each feature. Upper box plot whiskers represent the last data point within the range of the 75% quantile + 1.5 IQR. Lower box plot whiskers represent the last data point within the range of the 25% quantile − 1.5 IQR. Dots represent outliers (values smaller or larger than the median ± 1.5-times the interquartile range). Boxes with different letters are significantly different based on Fisher's least significant difference mean separation test ($P < 0.05$).

need to develop a well-characterized experimental system that facilitates follow-up investigations, especially of how root system adaptations can be integrated with tolerance mechanisms. Standardization of growth conditions is important because of evidence of the interactive effects of the P availability and plant response in modulating As uptake and accumulation. Standardization of experimental procedures and an understanding of root system adaptations to natural levels of As could lead to a more systematic exploitation of genome-wide techniques and characterization of the molecular basis of reduced As uptake in plants.

References Cited

Adalsteinsson S, Jensén P. 1988. Root development in winter wheat grown at different N/P supply: Root length patterns and N-P interactions in phosphate uptake. Physiol Plant. 72:271–278. https://doi.org/10.1111/j.1399-3054.1988.tb05833.x.

Bolan N, Mahimairaja S, Kunhikrishnan A, Choppala G. 2013. Phosphorus–arsenic interactions in variable-charge soils in relation to arsenic mobility and bioavailability. Sci Total Environ. 463: 1154–1162. https://doi.org/10.1016/j.scitotenv.2013.04.016.

Bianucci E, Furlan A, del Carmen Tordable M, Hernández LE, Carpena-Ruiz RO, Castro S. 2017. Antioxidant responses of peanut roots exposed to realistic groundwater doses of arsenate: Identification of glutathione S-transferase as a suitable biomarker for metalloid toxicity. Chemosphere. 181:551–561. https://doi.org/10.1016/j.chemosphere.2017.04.104.

Bilderback TE, Fonteno WC. 1987. Effects of container geometry and media physical properties on air and water volumes in containers. J Environ Hortic. 5:180–182. https://doi.org/10.24266/0738-2898-5.4.180.

Brackhage C, Huang JH, Schaller J, Elzinga EJ, Dudel EG. 2014. Readily available phosphorous and nitrogen counteract for arsenic uptake and distribution in wheat (Triticum aestivum L.). Sci Rep. 4:4944. https://doi.org/10.1038/srep04944.

Chakrabarty D, Trivedi PK, Misra P, Tiwari M, Shri M, Shukla D, Kumar S, Rai A, Pandey A, Nigam D, Tripathi RD. 2009. Comparative transcriptome analysis of arsenate and arsenite stresses in rice seedlings. Chemosphere. 74:688–702. https://doi.org/10.1016/j.chemosphere.2008.09.082.

Chandrakar V, Naithani SC, Keshavkant S. 2016. Arsenic-induced metabolic disturbances and their mitigation mechanisms in crop plants: A review. Biologia. 71:367–377. https://doi.org/10.1515/biolog-2016-0052.

Dixit G, Singh AP, Kumar A, Mishra S, Dwivedi S, Kumar S, Trivedi PK, Pandey V, Tripathi RD. 2016. Reduced arsenic accumulation in rice (Oryza sativa L.) shoot involves sulfur mediated improved thiol metabolism, antioxidant system and altered arsenic transporters. Plant Physiol Biochem. 99:86–96. https://doi.org/10.1016/j.plaphy.2015.11.005.

Duan GL, Liu WJ, Chen XP, Hua Y, Zhu YG. 2013. Association of arsenic with nutrient elements in rice plants. Metallomics. 5:5784–5792. https://doi.org/10.1039/c3mt20277a.

Elias M, Wellner A, Goldin-Azulay K, Chabriere E, Vorholt JA, Erb TJ, Tawfik DS. 2012. The molecular basis of phosphate discrimination in arsenate-rich environments. Nature. 491:134–137. https://doi.org/10.1038/nature11517.

Evans G, Evans J, Redman A, Johnson N, Foust RD. 2005. Unexpected beneficial effects of arsenic on corn roots grown in culture. Environ Chem. 23:167–170. https://doi.org/10.1071/EN05046.

Golombek SD, Johansen C. 1997. Effect of soil temperature on vegetative and reproductive growth and development in three Spanish genotypes of peanut (Arachis hypogaea L.). Peanut Sci. 24:67–72. https://doi.org/10.3146/i0095-3679-24-2-1.

Gregory PJ, Wojciechowski T. 2020. Root systems of major tropical root and tuber crops: Root architecture, size, and growth and initiation of storage organs. Adv Agron. 161:1–25. https://doi.org/10.1016/bs.agron.2020.01.001.

Griffiths M, Mellor N, Sturrock CJ, Atkinson BS, Johnson J, Mairhofer S, York LM, Atkinson JA, Soltaninejad M, Foulkes JF, Pound MP. 2022. X-ray CT reveals 4D root system development and lateral root responses to nitrate in soil. Plant Phenome J. 5:e20036. https://doi.org/10.1002/ppj2.20036.

Gupta K, Mishra K, Srivastava S, Kumar A. 2018. Cytotoxic assessment of chromium and arsenic using chromosomal behavior of root meristem in Allium cepa L. Bull Environ Contam Toxicol. 100:803–808. https://doi.org/10.1007/s00128-018-2344-2.

Hoagland DR, Arnon DI. 1950. The water-culture method for growing plants without soil. California Agric Exp Stn Res Bull. 347:3–32.

Huang TL, Nguyen QTT, Fu SF, Lin CY, Chen YC, Huang HJ. 2012. Transcriptomic changes and signalling pathways induced by arsenic stress in rice roots. Plant Mol Biol. 80: 587–608. https://doi.org/10.1007/s11103-012-9969-z.

Khattak RA, Page AL, Parker DR, Bakhtar D. 1991. Accumulation and interactions of arsenic, selenium, molybdenum and phosphorus in Alfalfa. J Environ Qual. 20:165–168. https://doi.org/10.2134/jeq1991.00472425002000010026x.

Kumar V, Vogelsang L, Schmidt RR, Sharma SS, Seidel T, Dietz KJ. 2020. Remodeling of root growth under combined arsenic and hypoxia stress is linked to nutrient deprivation. Front Plant Sci. 11:569687. https://doi.org/10.3389/fpls.2020.569687.

Kumari A, Pandey N, Pandey-Rai S. 2017. Protection of Artemisia annua roots and leaves against oxidative stress induced by arsenic. Biol Plant. 61:367–377. https://doi.org/10.1007/s10535-016-0686-3.

LaBonte DR, Villordon AQ, Smith T, Clark CA (inventors). 2013. Sweetpotato plant named '07-146'. Board of Supervisors of Louisiana State University and Agricultural and Mechanical College through the LSU AgCenter (assignee). US Patent PP23,785 P3. (Filed 22 Nov 2022, granted 30 Jul 2023).

López-Bucio J, Hernández-Abreu E, Sánchez-Calderón L, Nieto-Jacobo MF, Simpson J, Herrera-Estrella L. 2002. Phosphate availability alters architecture and causes changes in hormone sensitivity in the Arabidopsis root system. Plant Physiol. 129:244–256. https://doi.org/10.1104/pp.010934.

Lowe SB, Wilson LA. 1974. Comparative analysis of tuber development in six sweet potato (Ipomoea batatas (L.) Lam) cultivars: 1. Tuber initiation, tuber growth and partition of assimilate. Ann Bot. 38:307–317. https://doi.org/10.1093/oxfordjournals.aob.a084814.

Ma J, Aloni R, Villordon A, Labonte D, Kfir Y, Zemach H, Schwartz A, Althan L, Firon N. 2015. Adventitious root primordia formation and development in stem nodes of 'Georgia Jet' sweetpotato, Ipomoea batatas. Am J Bot. 102:1040–1049. https://doi.org/10.3732/ajb.1400505.

Mulkey WA, Hernandez JH. 1994. Louisiana's sweetpotato foundation seed program. Hort-Technology. 4:228–230. https://doi.org/10.21273/HORTTECH.4.3.228.

Nakatani M, Watanabe Y. 1986. Effects of soil temperatures on the rooting of cut-sprouts of sweet potato (Ipomoea batatas Lam.): I. Optimum soil temperature for rooting and effects of high soil temperatures on the physiological and anatomical characteristics of roots. Proc Crop Sci Soc Jpn. 55:208–216. https://doi.org/10.1626/jcs.55.208.

Navarro C, Navarro MA, Leyva A. 2022. Arsenic perception and signaling: The yet unexplored world. Front Plant Sci. 13:993484. https://doi.org/10.3389/fpls.2022.993484.

Panda SK, Upadhyay RK, Nath S. 2010. Arsenic stress in plants. J Agron Crop Sci. 196:161–174. https://doi.org/10.1111/j.1439-037X.2009.00407.x.

Piacentini D, Corpas FJ, D'Angeli S, Altamura MM, Falasca G. 2020. Cadmium and arsenic-induced-stress differentially modulates Arabidopsis root architecture, peroxisome distribution, enzymatic activities and their nitric oxide content. Plant Physiol Biochem. 148:312–323. https://doi.org/10.1016/j.plaphy.2020.01.026.

Piršelová B, Galuščáková Ľ, Lengyelová L, Kubová V, Jandová V, Hegrová J. 2022. Assessment of the hormetic effect of arsenic on growth and physiology of two cultivars of maize (Zea mays L.). Plants. 11:3433. https://doi.org/10.3390/plants11243433.

Pita-Barbosa A, Gonçalves EC, Azevedo AA. 2015. Morpho-anatomical and growth alterations induced by arsenic in Cajanus cajan (L.) DC (Fabaceae). Environ Sci Pollut Res Int. 22:11265–11274. https://doi.org/10.1007/s11356-015-4342-9.

Postma, JA, Dathe A, Lynch JP. 2014. The optimal lateral root branching density for maize depends on nitrogen and phosphorus availability. Plant Physiol. 166:590–602. https://doi.org/10.1104/pp.113.233916.

Punshon T, Jackson BP, Meharg AA, Warczack T, Scheckel K, Guerinot ML. 2017. Understanding arsenic dynamics in agronomic systems to predict and prevent uptake by crop plants. Sci Total Environ. 581:209–220. https://doi.org/10.1016/j.scitotenv.2016.12.111.

R Development Core Team. 2019. R: A language and environment for statistical computing. R Foundation for Statistical Computing, Vienna, Austria.

Rai R, Pandey S, Rai SP. 2011. Arsenic-induced changes in morphological, physiological, and biochemical attributes and artemisinin biosynthesis in Artemisia annua, an antimalarial plant. Ecotoxicology. 20:1900–1913. https://doi.org/10.1007/s10646-011-0728-8.

Rolston LH, Clark CA, Cannon JM, Randle WM, Riley EG, Wilson PW, Robbins ML. 1987. 'Beauregard' sweet potato. HortScience. 22:1338–1339. https://doi.org/10.21273/HORTSCI.22.6.1338.

Ronzan M, Piacentini D, Fattorini L, Caboni E, Eiche E, Ziegler J, Hause B, Riemann M, Betti C, Altamura MM, Falasca G. 2019. Auxin-jasmonate crosstalk in Oryza sativa L. root system formation after cadmium and/or arsenic exposure. Environ Exp Bot. 165:59–69. https://doi.org/10.1016/j.envexpbot.2019.05.013.

Rubinigg M, Wenisch J, Elzenga JTM, Stulen I. 2004. NaCl salinity affects lateral root development in Plantago maritima. Funct Plant Biol. 31:775–780. https://doi.org/10.1071/FP03222.

Schneider CA, Rasband WS, Eliceiri KW. 2012. NIH Image to ImageJ: 25 years of image analysis. Nat Methods. 9:671–675. https://doi.org/10.1038/nmeth.2089.

Seethepalli A, York LM. 2020. RhizoVision Explorer - interactive software for generalized root image analysis designed for everyone. 2.0.2. http://doi.org/10.5281/zenodo.4095629.

Singh N, Gaddam SR, Singh D, Trivedi PK. 2021. Regulation of arsenic stress response by ethylene biosynthesis and signaling in Arabidopsis thaliana. Environ Exp Bot. 185:104408. https://doi.org/10.1016/j.envexpbot.2021.104408.

Spagnoletti F, Lavado RS. 2015. The arbuscular mycorrhiza Rhizophagus intraradices reduces the negative effects of arsenic on soybean plants. Agronomy. 5:188–199. https://doi.org/10.3390/agronomy5020188.

Srivastava S, Pathare VS, Sounderajan S, Suprasanna P. 2019. Nitrogen supply influences arsenic accumulation and stress responses of rice (Oryza sativa L.) seedlings. J Hazard Mater. 367:599–606. https://doi.org/10.1016/j.jhazmat.2018.12.121.

Tang Z, Zhao FJ. 2021. The roles of membrane transporters in arsenic uptake, translocation and detoxification in plants. Crit Rev Environ Sci Technol. 51:2449–2484. https://doi.org/10.1080/10643389.2020.1795053.

Tawfik DS, Viola RE. 2011. Arsenate replacing phosphate: Alternative life chemistries and ion promiscuity. Biochem. 50:1128–1134. https://doi.org/10.1021/bi200002a.

Tripathi DK, Rai P, Guerriero G, Sharma S, Corpas FJ, Singh VP. 2021. Silicon induces adventitious root formation in rice under arsenate stress with involvement of nitric oxide and indole-3-acetic acid. J Expt Bot. 72:4457–4471. https://doi.org/10.1093/jxb/eraa488.

Tu S, Ma LQ. 2003. Interactive effects of pH, arsenic and phosphorus on uptake of As and P and growth of the arsenic hyperaccumulator Pteris vittata L. under hydroponic conditions. Environ Exp Bot. 50:243–251. https://doi.org/10.1016/S0098-8472(03)00040-6.

Villordon A, Gregorie JC, LaBonte D. 2020. Variation in phosphorus availability, root architecture attributes, and onset of storage root formation among sweetpotato cultivars. HortScience. 55:1903–1922. https://doi.org/10.21273/HORTSCI15358-20.

Villordon A, Clark C. 2018. Variation in root architecture attributes at the onset of storage root formation among resistant and susceptible sweetpotato cultivars infected with Meloidogyne incognita. HortScience. 53:1924–1929. https://doi.org/10.21273/HORTSCI10746-18.

Villordon A, Clark C. 2014. Variation in virus symptom development and root architecture attributes at the onset of storage root initiation in 'Beauregard' sweetpotato plants grown with or without nitrogen. PLoS One. 9:e107384. https://doi.org/10.1371/journal.pone.0107384.

Villordon A, Labonte D, Firon N, Carey E. 2013. Variation in nitrogen rate and local availability alter root architecture attributes at the onset of storage root initiation in 'Beauregard' sweetpotato. HortScience. 48:808–815. https://doi.org/10.21273/HORTSCI.48.6.808.

Villordon A, LaBonte D, Solis J, Firon N. 2012. Characterization of lateral root development at the onset of storage root initiation in 'Beauregard' sweetpotato adventitious roots. HortScience. 47:961–968. https://doi.org/10.21273/HORTSCI.47.7.961.

Villordon A, LaBonte D, Firon N, Kfir Y, Pressman E, Schwartz A. 2009. Characterization of adventitious root development in sweetpotato. HortScience. 44:651–655. https://doi.org/10.21273/HORTSCI.44.3.651.

Wagner K, Krause K, David A, Kai M, Jung EM, Sammer D, Kniemeyer O, Boland W, Kothe E. 2016. Influence of zygomycete-derived D'orenone on IAA signalling in Tricholoma-spruce ectomycorrhiza. Environ Microbiol. 18:2470–2480. https://doi.org/10.1111/1462-2920.13160.

Wang P, Xu X, Tang Z, Zhang W, Huang XY, Zhao FJ. 2018. OsWRKY28 regulates phosphate and arsenate accumulation, root system architecture and fertility in rice. Front Plant Sci. 9:1330. https://doi.org/10.3389/fpls.2018.01330.

Wickham H. 2009. ggplot2: Elegant graphics for data analysis. Springer, New York, NY, USA. https://doi.org/10.1007/978-3-319-24277-4.

Williamson LC, Ribrioux SP, Fitter AH, Leyser HO. 2001. Phosphate availability regulates root system architecture in Arabidopsis. Plant Physiol. 126:875–882. https://doi.org/10.1104/pp.126.2.875.

Wu J, Liang J, Björn LO, Li J, Shu W, Wang Y. 2022. Phosphorus-arsenic interaction in the 'soil-plant-microbe' system and its influence on arsenic pollution. Sci Total Environ. 802:149796.

Xu W, Dai W, Yan H, Li S, Shen H, Chen Y, Xu H, Sun Y, He Z, Ma M. 2015. Arabidopsis NIP3; 1 plays an important role in arsenic uptake and root-to-shoot translocation under arsenite stress conditions. Mol Plant. 8:722–773.

Zhe C, Wei R, Xia YI, Qiang LI, Cai HG, Farhan A, Yuan LX, Mi GH, Pan QC, Chen FJ. 2023. Local nitrogen application increases maize post-silking nitrogen uptake of responsive genotypes via enhanced deep root growth. J Integr Agric. 22:235–250. https://doi.org/10.1016/j.jia.2022.07.003.